A FLEXIBLE WAVEFIELD SIMULATION METHOD FOR LAYERED VISCOELASTIC MEDIA WITH DIPPING INTERFACES

CHAO WANG[1], JINGHUAI GAO[1], WEI ZHAO[2] and HUIQUN YANG[1]

[1] *School of Electronic and Information Engineering, Xi'an Jiaotong University, 710049, Xi'an, P.R. China. srmn28@163.com*
[2] *Research Center of China Offshore Corporation, 100027, Beijing, P.R. China.*

(Received January 12, 2011; revised version accepted September 5, 2011)

ABSTRACT

Wang, C., Gao, J., Zhao, W. and Yang, H.Q., 2011. A flexible wavefield simulation method for layered viscoelastic media with dipping interfaces. *Journal of Seismic Exploration*, 20: 309-329.

Partial wavefield simulation is very useful in seismic interpretation and inversion. In this work, we propose a flexible and fast method for simulating seismic wave propagation in dipping layered viscoelastic media. This method can effectively calculate various partial wavefields, e.g., primary reflected P-waves or primary reflected S-waves, P-S or S-P converted waves, and the multiples which we are interested in. Since the vector wave equations are independent of the coordinate system, we alternately study wave propagation in global and local coordinate systems. Firstly, for a single dipping interface, the reflection and transmission coefficients of plane waves and the expressions of secondary waves are obtained by coordinate transformation. Then, the reflection and transmission coefficients of multi-layered media with dipping interfaces are obtained by a recursive approach. Lastly, a fast integral method is used to synthesize the wavefield for a point source, and a novel integral path is chosen through comparison. Analysis shows that this method is stable for all frequencies and slownesses. Numerical examples and a comparison with a finite difference solution demonstrate that our method is effective.

KEY WORDS: partial wavefield, simulation, dipping interface, viscoelastic.

INTRODUCTION

The complete seismic wavefield is complex as various types of waves interfere with each other. However, for some applications, we are only interested in a partial wavefield. For instance, for amplitude variations with offset (AVO) interpretation (Steven and Robert, 1989), we just need the primary reflected waves, and for multiple prediction (Kroode, 2002), we are often only

0963-0651/11/$5.00

interested in the multiples of the objective layer. Another important application of partial wavefield simulation is the identification of specific events on a seismic record. These partial wavefields are usually blurred by other components. It is difficult to extract a partial wavefield from the complete wavefield. Therefore, simulating various partial wavefields may be of great practical importance.

Many seismic modeling methods are based on the assumption of a stratified structure of the earth. For example, the reflectivity method is efficient for calculating the complete or partial wavefield of horizontal layered media (Aki and Richards, 2002; Kennett, 1983; Müller, 1985). The wavefield extrapolation method (Berkhout, 1982; Bourbie, 1983) can be used to simulate wave propagation in elastic media with dipping interfaces, but the horizontal interface is required when the media is viscoelastic. Improved generalized reflectivity method (Chen, 1990, 1996) and boundary element approach (Ge and Chen, 2007) were proposed to simulate wave propagation in irregularly stratified elastic models. However, the methods mentioned above are not effective for simulating a partial wavefield while the media is both viscoelastic and has dipping interfaces.

In recent decades, many other approaches have been developed for complex media (Carcione and Hermann, 2002). The most used numerical methods, such as the finite difference method (Stekl and Pratt, 1998), finite element method (Martin and Michael, 2006; Becache et al., 2004), and spectral element method, can calculate the complete wavefield of very complex models, but they are expensive in terms of computer time and are not effective in simulating the partial wavefields. The high-frequency asymptotic methods, such as ray theory and Gaussian beam, are able to simulate various partial wavefields, but they are only appropriate for handing wave propagation under relatively high frequency.

Although the real media is complex, the layered model is still a preferable approximation for many applications. Layered model is simple and therefore, some fast and exact methods can be developed to simulate wave propagation. Consequently, based on these forward modeling methods, some seismic attributes' inversion algorithms, for example, interval velocity inversion or interval Q inversion, can be proposed. In this paper, we propose a one-way wave propagation method to simulate seismic wave propagation in multi-layered viscoelastic media with dipping interfaces in the frequency wavenumber domain.

METHOD

The definitions of the main symbols that are used in this paper are listed in Table 1.

Table 1. Definitions of symbols used in this paper.

Symbol	Definition
XOZ	Global Cartesian coordinate system.
$\hat{X}\hat{O}\hat{Z}$	Local Cartesian coordinate system.
$\hat{}$	The variables marked with superscript $\hat{}$ belong to the local coordinate system; otherwise, they belong to the global coordinate system.
p_i, $\hat{p}_i$, q_i, $\hat{q}_i$	The horizontal and vertical slownesses in the i-th layer.
ϕ_i, $\hat{\phi}_i$, ψ_i, $\hat{\psi}_i$	The downgoing P-waves and SV-waves in the i-th layer.
$\phi'_{i,n}$, $\hat{\phi}'_{i,n}$, $\psi'_{i,n}$, $\hat{\psi}'_{i,n}$	The upgoing P-waves and SV-waves. The first subscript indicates the layer in which the wave is traveling and the second subscript indicates the interface by which the wave is reflected. Remark: The second subscript is omitted for the case of a single interface.
$R^d_{pp,i}$, $\hat{R}^d_{pp,i}$, $T^d_{ps,i}$, $\hat{T}^d_{ps,i}$	The reflection and transmission coefficients for the downgoing incident wave. The first and second subscripts indicate the types of the incident and secondary waves, respectively, and the third subscript indicates the i-th interface. Remark: The third subscript is omitted for the case of a single interface.
$T^u_{ps,i}$, $\hat{T}^u_{ps,i}$	The transmission coefficients for the upgoing incident wave. Subscripts are the same as above. Remark: The third subscript is omitted for the case of a single interface.

Reflection and transmission at a dipping interface

In this study, we solve the problem for 2D P-SV wave propagation, but a similar technique can be used in the SH case or the acoustic-wave case as well. We start with the case of two homogeneous half-spaces separated by a dipping interface. As shown in Fig. 1, θ is the dipping angle of the interface, and the densities of medium I and medium II, respectively, and α_i and β_i (i = 1,2) the P- and S-velocities, respectively. Because we are dealing with viscoelastic media, all velocities should be complex and frequency-dependent. Several models relate the complex velocities to the frequency and quality factor Q (Toverud and Ursin, 2005). Here, the Kolsky-Futterman model is adopted:

$$1/c(\omega) = (1/c_r) + (1/\pi c_r Q_r)\ln|\omega_r/\omega| + j\,\mathrm{sgn}(\omega)/2c_r Q_r \quad , \tag{1}$$

where ω is the angle frequency, c_r and Q_r are the reference velocity and quality factor at reference frequency ω_r, respectively, j is an imaginary unit.

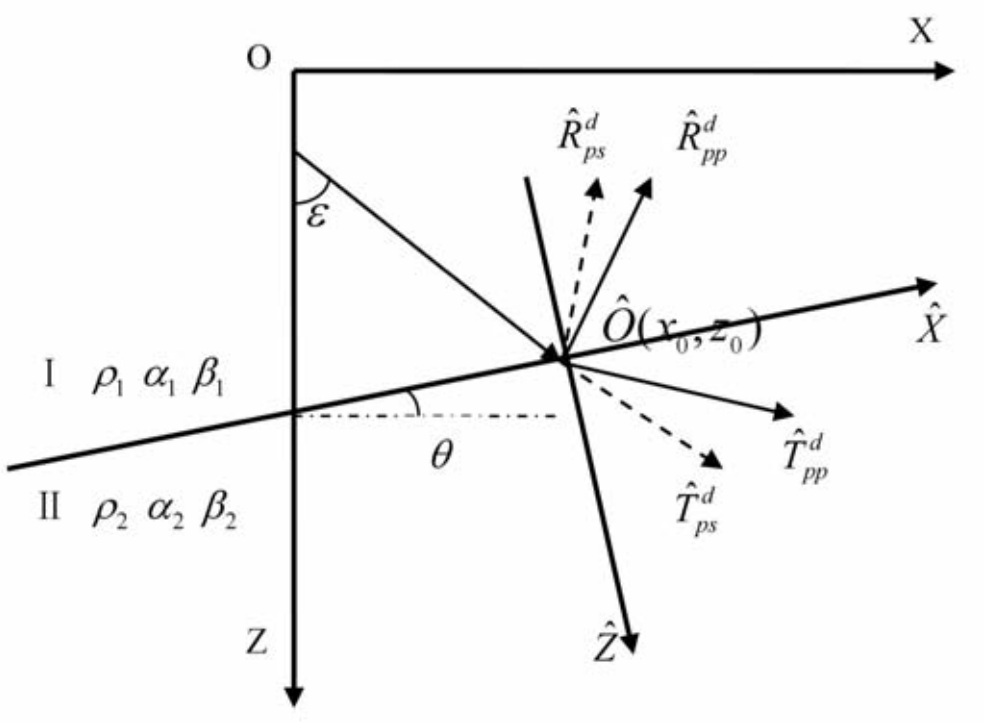

Fig. 1. Two half-spaces with a dipping interface. For a downgoing incident P- wave, there are four secondary waves.

Establishing two Cartesian coordinate systems (as shown in Fig. 1), a global coordinate system XOZ with its x-axis at the horizontal direction and a local coordinate system $\hat{X}\hat{O}\hat{Z}$ with its $\hat{x}$-axis on the dipping interface and its origin at (x_0,z_0) is seen. The two coordinate systems are then related through the following equations:

$$\begin{aligned} \hat{x} &= (x - x_0)\cos\theta + (z - z_0)\sin\theta \ , \\ \hat{z} &= -(x - x_0)\sin\theta + (z - z_0)\cos\theta \ . \end{aligned} \tag{2}$$

Through this paper, the variables marked with superscript $\hat{}$ belong to the local coordinate system $\hat{X}\hat{O}\hat{Z}$, if otherwise they belong to the global coordinate system XOZ.

In the local coordinate system, if there is an incident plane P-wave $\hat{\phi}_1$ traveling downwards in medium I, the secondary waves produced at the interface are the reflected P-wave $\hat{\phi}_1'$ and SV-wave $\hat{\psi}_1'$ and the transmitted P-wave $\hat{\phi}_2$ and SV-wave $\hat{\psi}_2$. It is easy to write out their expressions:

$$\hat{\phi}_1 = \exp[j\omega(\hat{p}\hat{x} + \hat{q}_1\hat{z})] \quad , \tag{3.1}$$

$$\hat{\phi}_1' = \hat{R}_{pp}^d \cdot \exp[j\omega(\hat{p}\hat{x} - \hat{q}_1\hat{z})] \quad , \tag{3.2}$$

$$\hat{\psi}_1' = \hat{R}_{ps}^d \cdot \exp[j\omega(\hat{p}\hat{x} - \hat{q}_1'\hat{z})] \quad , \tag{3.3}$$

$$\hat{\phi}_2 = \hat{T}_{pp}^d \cdot \exp[j\omega(\hat{p}\hat{x} + \hat{q}_2\hat{z})] \quad , \tag{3.4}$$

$$\hat{\psi}_2 = \hat{T}_{ps}^d \cdot \exp[j\omega(\hat{p}\hat{x} - \hat{q}_2'\hat{z})] \quad , \tag{3.5}$$

where the incident P-wave has a unit of the potential amplitude. $\hat{R}_{pp}^d$, $\hat{R}_{ps}^d$, $\hat{T}_{pp}^d$ and $\hat{T}_{ps}^d$ are the reflection and transmission coefficients. The superscript d indicates that the incident wave is a downgoing incident wave, the first and second subscripts indicate the types of the incident wave and secondary wave, respectively. All waves' horizontal slownesses relative to $\hat{X}\hat{O}\hat{Z}$ are $\hat{p}$, and vertical slownesses are $\hat{q}_1$, $\hat{q}_2$, $\hat{q}_1'$, $\hat{q}_2'$, respectively. For viscoelastic media, one must take some care to choose the signs of the complex vertical slownesses. Krebes and Daley (2007) regarded that it is better to take the signs of the real part and imaginary part as positive at all times.

In $\hat{X}\hat{O}\hat{Z}$, the interface is parallel to the $\hat{x}$-axis. For this case, a number of algorithms have been developed to calculate the coefficients $\hat{R}_{pp}^d$, $\hat{R}_{ps}^d$, $\hat{T}_{pp}^d$ and $\hat{T}_{ps}^d$ for details, one can refer to Aki and Richards (2002), Kennett (1983) and Müller (1985) as they are not described here.

Our aim is to obtain the reflection and transmission coefficients in the global coordinate system. As the vector wave equations are independent of the coordinate system, they have the same forms in different two-dimensional coordinate systems. Therefore, all waves in XOZ should have the same forms as in $\hat{X}\hat{O}\hat{Z}$. Transforming eqs. (3.1) - (3.5) into XOZ by inserting eq. (2) into eqs. (3.1) - (3.5), after rearranging, we obtain the incident P-wave and transmitted P-wave in the global coordinate system:

$$\phi_1 = A_1 \exp[j\omega\{(\hat{p}\cos\theta - \hat{q}_1\sin\theta)x + (\hat{p}\sin\theta + \hat{q}_1\cos\theta)z\}] \quad , \tag{4}$$

$$\phi_2 = A_2 \exp[j\omega\{(\hat{p}\cos\theta - \hat{q}_2\sin\theta)x + (\hat{p}\sin\theta + \hat{q}_2\cos\theta)z\}] \quad , \tag{5}$$

where

$$A_1 = \exp[-j\omega\{(\hat{p}\cos\theta - \hat{q}_1\sin\theta)x_0 + (\hat{p}\sin\theta + \hat{q}_1\cos\theta)z_0\}] \quad , \tag{6}$$

$$A_2 = \hat{T}_{pp}^d \exp[-j\omega\{(\hat{p}\cos\theta - \hat{q}_2\sin\theta)x_0 + (\hat{p}\sin\theta + \hat{q}_2\cos\theta)z\}] \quad . \tag{7}$$

The ratio of A_2 to A_1, which are independent of the coordinate variable (x,z), give out the P-wave transmission coefficient in the global coordinate

system:

$$T_{pp}^{d} = A_2/A_1 = \hat{T}_{pp}^{d}\exp[j\omega(\hat{q}_2 - \hat{q}_1)(x_0\sin\theta - z_0\cos\theta)] \quad . \tag{8}$$

Accordingly, the transmitted P-wave for a normalized incident P-wave can be written as:

$$\phi_2 = T_{pp}^{d}\exp[j\omega\{(\hat{p}\cos\theta - \hat{q}_2\sin\theta)x + (\hat{p}\sin\theta + \hat{q}_2\cos\theta)z\}] \quad . \tag{9}$$

Similarly, the reflected P-wave and the reflected and transmitted SV-waves can be written as:

$$\phi_1' = R_{pp}^{d}\exp[j\omega\{(\hat{p}\cos\theta + \hat{q}_1\sin\theta)x - (-\hat{p}\sin\theta + \hat{q}_1\cos\theta)z\}] \ , \tag{10.1}$$

$$\psi_1' = R_{ps}^{d}\exp[j\omega\{(\hat{p}\cos\theta + \hat{q}_1'\sin\theta)x - (-\hat{p}\sin\theta + \hat{q}_1'\cos\theta)z\}] \ , \tag{10.2}$$

$$\psi_2 = T_{ps}^{d}\exp[j\omega\{(\hat{p}\cos\theta - \hat{q}_2'\sin\theta)x + (\hat{p}\sin\theta + \hat{q}_2'\cos\theta)z\}] \ , \tag{10.3}$$

$$R_{pp}^{d} = \hat{R}_{pp}^{d}\exp[j\omega 2\hat{q}_1(-x_0\sin\theta + z_0\cos\theta)] \ , \tag{11.1}$$

$$R_{ps}^{d} = \hat{R}_{ps}^{d}\exp[j\omega(\hat{q}_1' + \hat{q}_1)(-x_0\sin\theta + z_0\cos\theta)] \ , \tag{11.2}$$

$$T_{ps}^{d} = \hat{T}_{ps}^{d}\exp[j\omega(\hat{q}_2' - \hat{q}_1)(x_0\sin\theta - z_0\cos\theta)] \ . \tag{11.3}$$

For the case of an incident SV wave or the incident wave traveling upwards in medium II, the reflection and transmission coefficients and the expressions of all the secondary waves can be obtained with the same way as above. Here, we only give out the expression of the transmitted P-wave, while the incident wave is the P-wave that travels upwards in medium II:

$$\phi_1' = T_{pp}^{u}\exp[j\omega\{(\hat{p}\cos\theta + \hat{q}_1\sin\theta)x - (-\hat{p}\sin\theta + \hat{q}_1\cos\theta)z\}] \ , \tag{12}$$

$$T_{pp}^{u} = \hat{T}_{pp}^{u}\exp[j\omega(\hat{q}_2 - \hat{q}_1)(x_0\sin\theta - z_0\cos\theta)] \ , \tag{13}$$

where, the superscript 'u' of T_{pp}^{u} means that the incident wave is upgoing.

It must be noted that these reflection and transmission coefficients for a dipping interface in XOZ are different from the conventional reflection and transmission coefficients. The former are dependent on the position and dipping angle of the interface, whereas the latter are independent of the position and dipping angle of the interface. Furthermore, all the expressions of secondary waves have very simple forms and their exponential terms only have a relation to the parameters of the current media in which they are propagating. Therefore, it is very convenient to extend the case of a single dipping interface to the case of layered media with many different dipping interfaces.

Partial wavefield simulation of layered media with dipping interfaces

For horizontal layered media, waves have the same horizontal slowness in all the layers. However, the horizontal slowness will be changed if a wave were to meet a dipping interface. Thus, we must extrapolate the wave, by each of the layers, one after the other in dipping layered media. Though it is complicated, it is advantageous for us to choose the type (reflected or transmitted and P or S) of the wave in each layer. Therefore, we can simulate various partial wavefields, respectively.

Below, we mainly illustrate the algorithm for simulating primary reflected waves. Other wavefields can be treated in a similar way. Fig. 2 illustrates a model with N dipping layers, the first and last layers are infinite half-spaces. The dipping angle of interface i is θ_i, the density, P-wave velocity and SV-wave velocity of medium i are ρ_i, α_i, β_i (i = 1,2,...,N). Receivers are set in the first layer with z = 0.

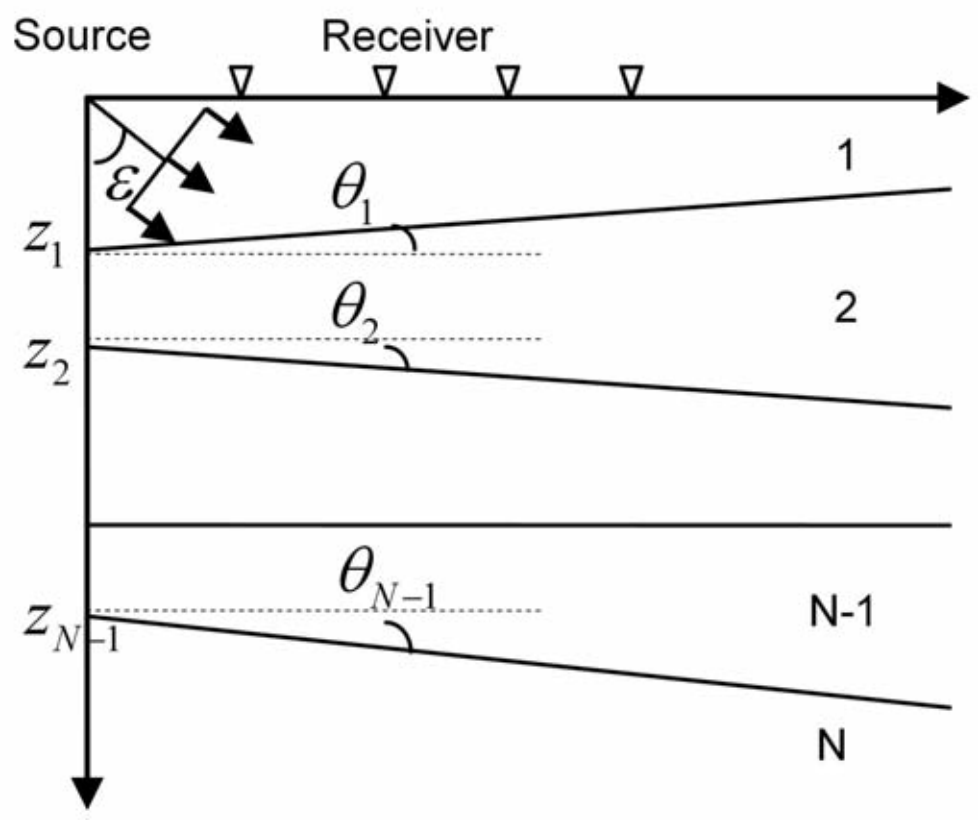

Fig. 2. Multi-layered model with dipping interfaces.

Assume that the incident wave is a P-wave starting from the origin and the horizontal and vertical slownesses are p_1 and q_1:

$$\phi_1 = \exp[j\omega(p_1 x + q_1 z)] \quad . \tag{14}$$

This incident wave is extrapolated one layer by one layer. The procedure for each interface met by the wave is illustrated in Fig. 3. The main steps may be described as follows:

1. For the downgoing wave, once an interface i is met, we establish a local coordinate system $\hat{X}\hat{O}\hat{Z}$ with its $\hat{x}$-axis on the interface i and its origin at the point ($x_i = 0$,z), which is the crosspoint of the interface i and the z-axis of the global coordinate system. Subsequently, the incident wave ϕ_i is transformed into the local coordinate system, getting $\hat{\phi}_i$.

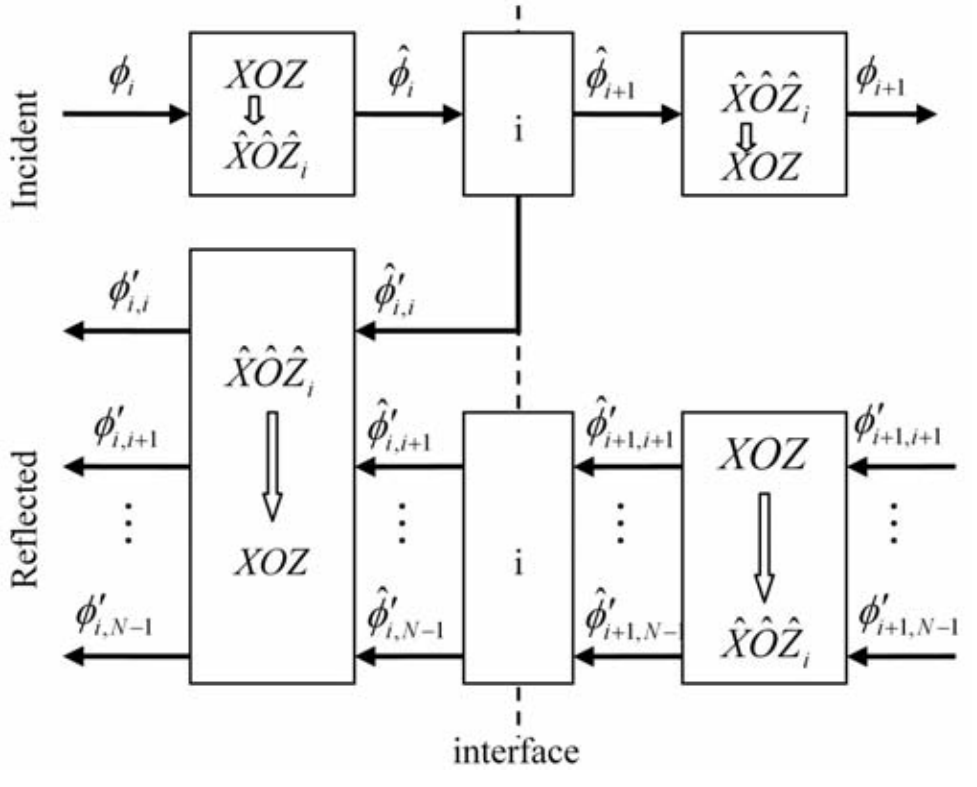

Fig. 3. Schematic illustration of the recursive procedure for the transmitted and reflected waves. The hollow arrow means coordinate transformation, the subscript i of $\hat{X}\hat{O}\hat{Z}_i$ indicates that the $\hat{x}$-axis of this local coordinate system is on the i-th interface, the first subscripts of all waves indicate the layer in which layer they are traveling and the second subscript of the reflected waves indicate the interface from which they are reflected.

2. The conventional reflection and transmission coefficients ($\hat{R}^d_{pp,i}$, $\hat{T}^d_{pp,i}$) and the secondary waves ($\hat{\phi}'_{i,i}$, $\hat{\phi}_{i+1}$) are computed in the local coordinate system (the first subscript of $\hat{\phi}'_{i,i}$ indicates the layer in which the wave is traveling and the second subscript indicates the interface by which the upgoing wave is reflected).

3. Following, the secondary waves ($\hat{\phi}'_{i,i}$, $\hat{\phi}_{i+1}$) are transformed back into the global coordinate system. Getting the reflection and transmission coefficients ($R^d_{pp,i}$, $T^d_{pp,i}$) and the secondary waves ($\phi'_{i,i}$, ϕ_{i+1}).

4. The reflected wave $\phi'_{i,i}$ will be extrapolated upwards to the surface. Only the transmitted wave is chosen on each interface in this process.

5. The transmitted wave ϕ_{i+1} will be extrapolated downwards. When another interface is met, return to step 1.

By this way, the primary downgoing wave in the nth layer can be written as:

$$\phi_n = \prod_{i=1}^{n-1} T^d_{pp,i} \exp[j\omega(p_n x + q_n z)] \quad , \quad (n = 2,3,\ldots,N) \tag{15}$$

where $T^d_{pp,i}$ is the downgoing transmission coefficients of the i-th interface, which follows from eq. (8) by replacing the parameters $\hat{T}^d_{pp},\theta$ by $\hat{T}^d_{pp,i},\theta_i$ and x_0, z_0, $\hat{q}_1$, $\hat{q}_2$ by x_i, z_i, $\hat{q}_i$, $\hat{q}_{i+1}$:

$$T^d_{pp,i} = \hat{T}^d_{pp,i} \exp[j\omega(\hat{q}_{i+1} - \hat{q}_i)(x_i \sin\theta_i - z_i \cos\theta_i)] \quad . \tag{16}$$

The horizontal and vertical slownesses for the downgoing wave can be obtained by the following recursive formula:

$$\begin{aligned}
p_i &= \hat{p}_i \cos\theta_{i-1} - \hat{q}_i \sin\theta_{i-1} \quad , \\
q_i &= \hat{p}_i \sin\theta_{i-1} + \hat{q}_i \cos\theta_{i-1} \quad , \\
\hat{p}_i &= \hat{p}_{i-1} \quad , \quad \hat{q}_i = \sqrt{(\alpha_i^{-2} - \hat{p}_i^2)} \quad , \quad (i = 2,3,\ldots,N) \\
\hat{p}_{i-1} &= p_{i-1} \cos\theta_{i-1} + q_{i-1} \sin\theta_{i-1} \quad .
\end{aligned} \tag{17}$$

We can also obtain the primary reflected wave that comes from the n-th interface:

$$\phi'_{1,n} = \prod_{i=1}^{n-1} T^u_{pp,i} \cdot R^d_{pp,n} \cdot \prod_{i=1}^{n-1} T^d_{pp,i} \cdot \exp[j\omega(p_1 x - q_1 z)] \quad , \tag{18}$$

where $T^u_{pp,i}$ is the upgoing transmission coefficient of the i-th interface and $R^d_{pp,n}$ the reflection coefficient of the n-th interface; they follow from eq. (13) and eq. (10.1), respectively. The horizontal and vertical slownesses for the upgoing wave can be obtained by the following recursive formula:

$$\begin{aligned} p_{i-1} &= \hat{p}_{i-1}\cos\theta_{i-1} + \hat{q}_{i-1}\sin\theta_{i-1} \ , \\ q_{i-1} &= -\hat{p}_{i-1}\sin\theta_{i-1} + \hat{q}_{i-1}\cos\theta_{i-1} \ , \\ \hat{p}_{i-1} &= \hat{p}_i \ , \quad \hat{q}_{i-1} = \sqrt{(\alpha_{i-1}^{-2} - \hat{p}_{i-1}^2)} \ , \quad (i = N-1,\ldots,1) \\ \hat{p}_i &= p_i\cos\theta_{i-1} - q_i\sin\theta_{i-1} \ . \end{aligned} \tag{19}$$

In eq. (18), replacing $R^d_{pp,n}$ with $R^d_{ps,n}$ and $T^u_{pp,i}$ with $T^u_{ss,i}$, we can obtain the P-S converted wave. In fact, we can decide which of the secondary waves (reflected or transmitted and P or S) should be chosen at each interface. Similar to the ray code (Červený, 2001), these choices can be indicated by using a chain of characters; e.g., the P-S converted wave coming from the second interface can be coded as (+P, +P, −S, −S), and the first multiples of the first layer can be coded as (+P, −P, +P, −P). Here, the + and − indicate the downgoing wave and upgoing wave, respectively; the P and S indicate the P-wave and S-wave, respectively. Choosing corresponding reflection and transmission coefficients in eq. (18) according to the code, we can get various partial wavefields.

Stability analysis

Here, we consider only the P-P transmission coefficient as an example. According to eq. (16), the i-th transmission coefficient in eq. (15) can be written as (take $x_i = 0$):

$$T^d_{pp,i} = \hat{T}^d_{pp,i}\exp[j\omega z_i\cos\theta_i(\hat{q}_i - \hat{q}_{i+1})] \ . \tag{20}$$

Because the imaginary part of $\hat{q}_{i+1}$ is positive and $z_i\cos\theta_i$ is positive real, the $\exp(-j\omega z_i\cos\theta_i\hat{q}_{i+1})$ in eq. (20) is exponentially increasing as ω is increasing. If we compute the value of $T^d_{pp,i}$ according to eq. (20) instantly, it will overflow for large ω. However, in the (i+1)-th transmission coefficient:

$$T^d_{pp,i+1} = \hat{T}^d_{pp,i+1}\exp[j\omega z_{i+1}\cos\theta_{i+1}(\hat{q}''_{i+1} - \hat{q}_{i+2})] \ , \tag{21}$$

there is an exponent term $\exp(j\omega z_{i+1}\cos\theta_{i+1}\hat{q}''_{i+1})$. The product of $\exp(-j\omega z_i\cos\theta_i\hat{q}_{i+1})$ and $\exp(j\omega z_{i+1}\cos\theta_{i+1}\hat{q}''_{i+1})$ is $\exp(j\omega z_{i+1}\cos\theta_{i+1}\hat{q}''_{i+1} - j\omega z_i\cos\theta_i\hat{q}_{i+1})$. The real part of the power of this exponent will be negative, so

this exponent is exponentially decreasing as ω is increasing. This is consistent with the attenuation characteristics of wave propagations in viscoelastic media.

Therefore, to avoid overflow, we record the powers of the exponent of eq. (16) instead of solely computing the value of the exponent term for each coefficient. Then all the recorded powers are summed up before calculating the exponent. Continuing like this, our method will be stable for all frequencies.

Integral path for point source

As a Weyl integral, the spherical wave can be represented by a superposition of plane waves (Aki, 2002). Thus, the wavefield excited by a point source can be expressed as a superposition of the plane waves, which have been discussed in the above sections.

$$P = (1/2\pi) \int_{\Gamma} A(p)\{\exp[j\omega p''x \pm j\omega q''z)]/-2jq\}dp \quad , \tag{22}$$

where A(p) is referred as the reflection or transmission function, Γ is the integral path. p, q are the horizontal and vertical slownesses of the plane wave at source, and p'', q'' are the horizontal and vertical slownesses at the receivers. We must keep in mind that the horizontal slowness is variational in dipping layered media.

Many integral paths can be chosen from the complex slowness plane. For elastic media, the path of Γ in Fig. 4(a) is usually used (Chapman, 1978; Fuchs and Müller, 1971), and the path of Γ' in Fig. 4(a) was used by Frazer and Gettrust (1984). These paths are slightly deviated from the real axis to avoid the poles. For viscoelastic media, because the poles lie in the first and third quadrants, the real axis can be chosen as the integral path. However, there will appear some undesired waves in the synthetic seismogram, as shown in Fig. 5(a). We then calculate eq. (22) along the path Γ_1 shown in Fig. 4(b) in the light of Frazer, and the synthetic seismogram is ideal, as shown in Fig. 5(b). However, the segment AB of Γ_1, which is dominant for the integral eq. (22), is on the real axis. It means that the wave will not attenuate while it propagates along the horizontal direction. This is in conflict with the viscoelasticity of viscoelastic media. Therefore, the path Γ_2 shown in Fig. 4(b) is chosen finally. The dipping angle for segment AB of Γ_2 is decided by the quality factor Q (AB will be slightly below the poles). Fig. 5(c) shows the comparison for the peak amplitude of the envelope of the synthetic seismograms with integral paths Γ_1 and Γ_2. We can see that the synthetic seismogram with Γ_2 has smaller peak at far offsets.

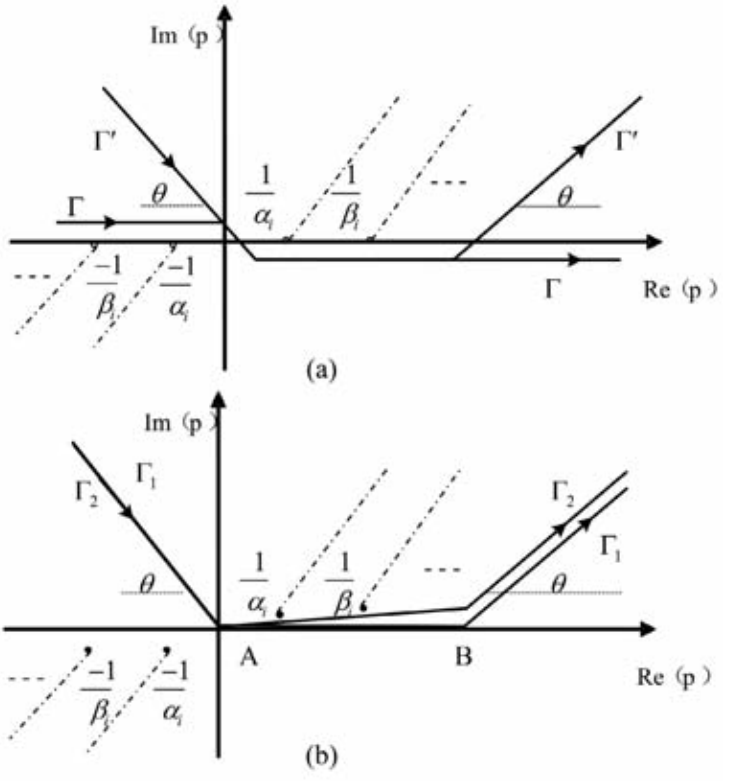

Fig. 4. Contours of integral path. $1/\alpha_i$ and $1/\beta_i$ are the slownesses of P-wave and S-wave, respectively. Before Γ turns into the first quadrant, Re(Γ) should be slightly greater than max(real($1/\beta_i$)).

Fast integral method

Eq. (22) is an oscillatory integral. For the standard trapezoidal method, the integration step size is in inverse proportion to max(ωx,ωz). Therefore, the step size must be very small when ω is large. In order to save computation time, the generalization of Filon's method (GFM) introduced by Frazer and Gettrust (1984) is adopted to evaluate this integral. We rewrite eq. (22) as:

$$P = (1/2\pi) \int_{\Gamma} f(p)\exp[sg(p)]dp \quad , \tag{23}$$

where

$$f(p) = -A(p)/2\pi \cdot 2jq \quad ,$$

$$s = j\omega \cdot \max(x,z) \quad ,$$

$$g(p) = (p''x - q''z)/\max(x,z) \quad .$$

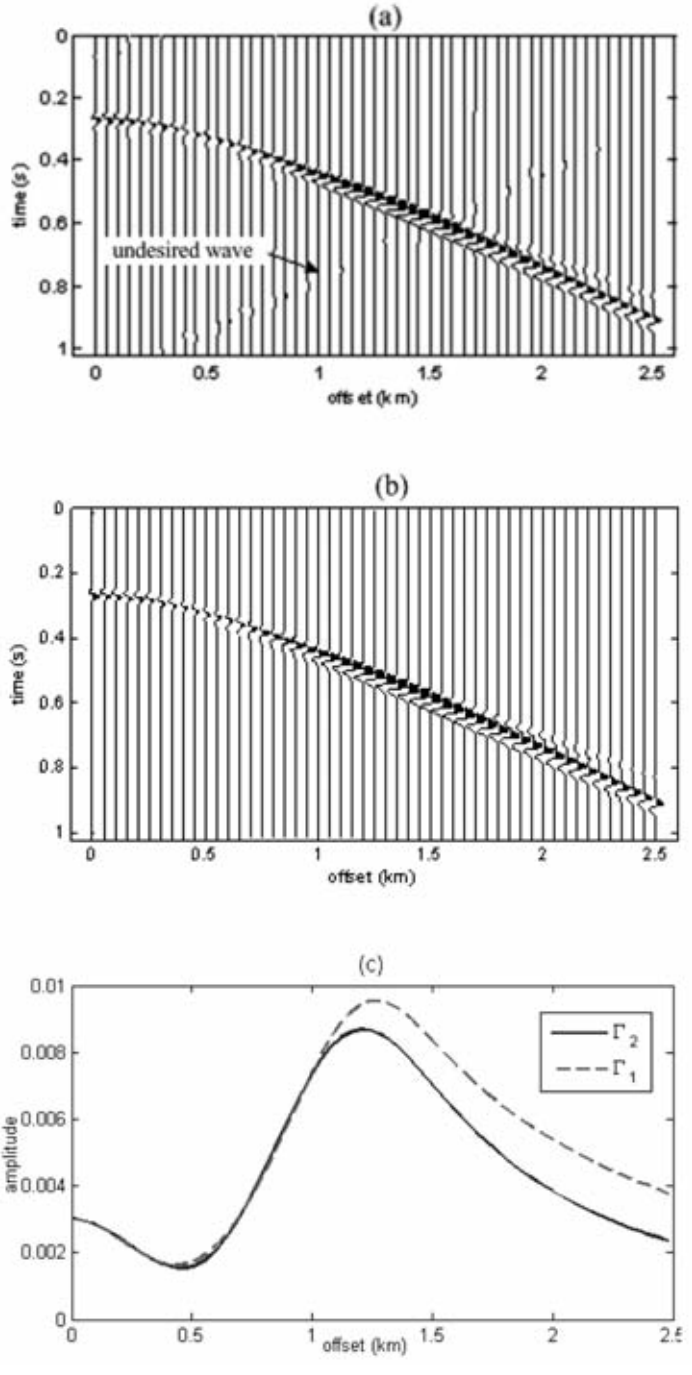

Fig. 5. Synthetic seismograms with the integral path along the real axis (a) and the contour Γ_1 (b). (c) The comparison for the peak amplitude of envelope of the synthetic seismograms with integral paths Γ_1 and Γ_2.

Accordingly, the rule of GFM is:

$$\int_a^b f(p)\exp[sg(p)]dp = \begin{cases} (\delta p/s\delta g)[\delta(fe^{sg}) - \delta(f)\delta(fe^{sg})/s\delta(g)] & \delta g \neq 0 \\ (\delta p/2)[f(a)e^{sg(a)} + f(b)e^{sg(b)})] & \delta g = 0 \end{cases} \quad (24)$$

where $b-a$ is the integration step size, for any function h, $\delta(h)$ means $h(b)-h(a)$. For GFM, the step size is in inverse proportion to $\sqrt{\max(\omega x, \omega z)}$.

NUMERICAL EXAMPLES

First, a synthetic seismogram of acoustic media is generated to test the capability of our method. The test model, as shown in Fig. 6(a), has a dipping layer between two half-spaces. The dipping angles of the two interfaces are 4 and 8 degrees, respectively. The parameters are relative to the reference frequency of 1 Hz. Fig. 6(b) shows the comparison of the synthetic reflected seismograms with the finite difference method and our method. We can see that both the amplitudes and arrival times are in good agreement. To indicate the wavefield characteristic caused by different Q, seismogram for $Q_1 = 1000$ is also calculated with our method and a careful comparison of individual traces with an offset of 100 m are shown in Fig. 7. For $Q_1 = 30$, the reflected wave from the upper interface has a larger amplitude than the case of $Q_1 = 1000$, and the wave from the second interface has a smaller amplitude, advanced travel-time and smaller dominant frequency than $Q_1 = 1000$. These phenomena are consistent with the theory.

Next, let us consider a viscoelastic-layered model with five interfaces. This model, shown in Fig. 8, is a simplified version of the left part of the Marmousi-2 model. There is a low-velocity layer in this model and the contrast of parameters is strong. The dipping angles for five interfaces are -5.12, -3.52, 0,0 and -9.92 degrees, respectively. A Ricker wavelet with a dominant frequency of 30 Hz is used as source and set at the origin (0, 0). The receivers are first set in the well with offset of 1 km and depth range of 0.5 - 2 km. Fig. 9(a) shows the x-component of the synthetic VSP seismogram, which includes the direct waves, primary reflected P-waves and converted S-waves. For comparison, Fig. 9(b) shows the x-component of the synthetic seismogram by the finite difference method. We can see that two seismograms have the same travel time and polarity for all waves. The primary reflected P-waves are too weak to be distinguished from other waves in Fig. 9. Therefore, some partial wavefields are solely generated by our method. Fig. 10(a), (b) and (c) show the x-component of direct waves, primary reflected P-waves and converted S-waves, respectively.

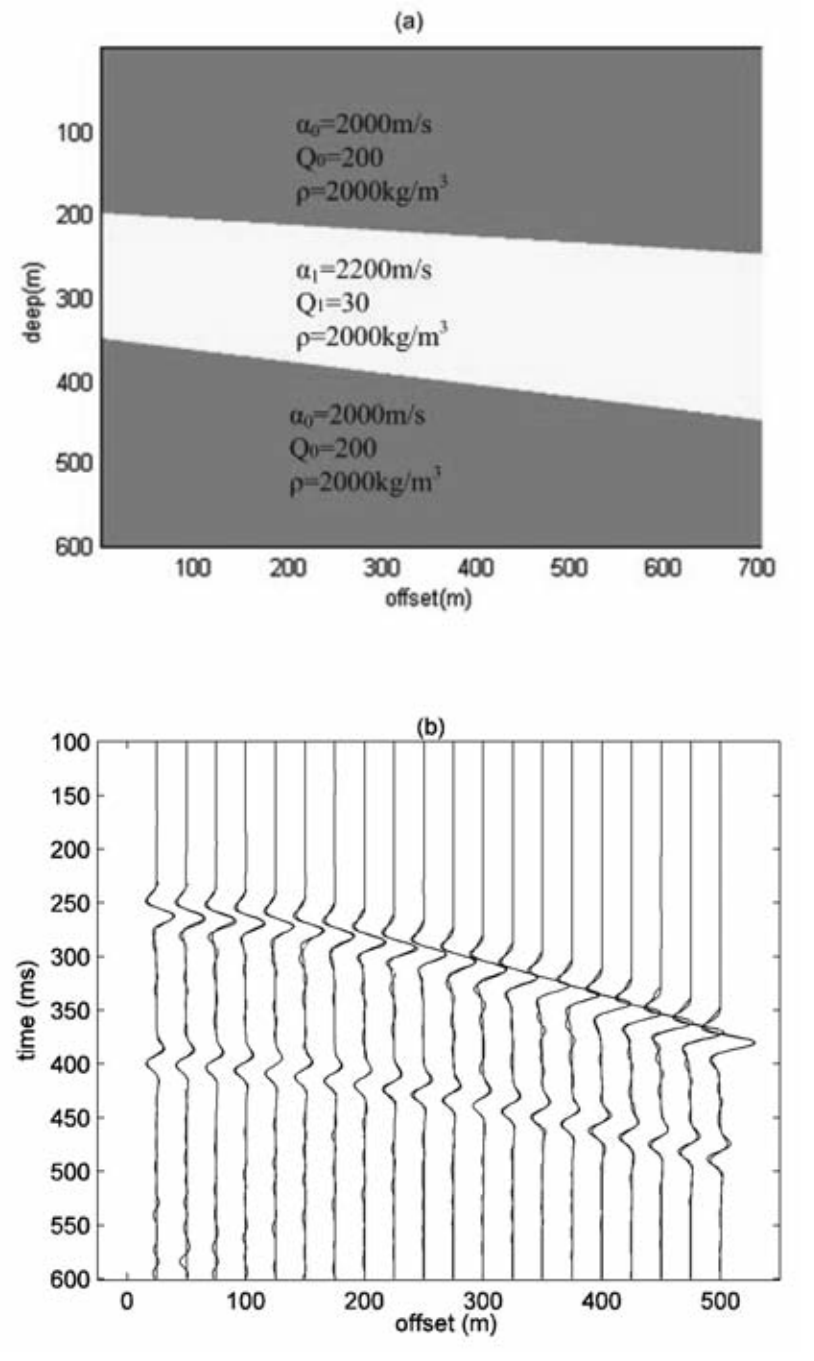

Fig. 6. (a) Acoustic media with a dipping layer between two half-spaces. (b) Comparison of the synthetic seismograms calculated by our method (solid lines) and by finite difference method (dashed lines).

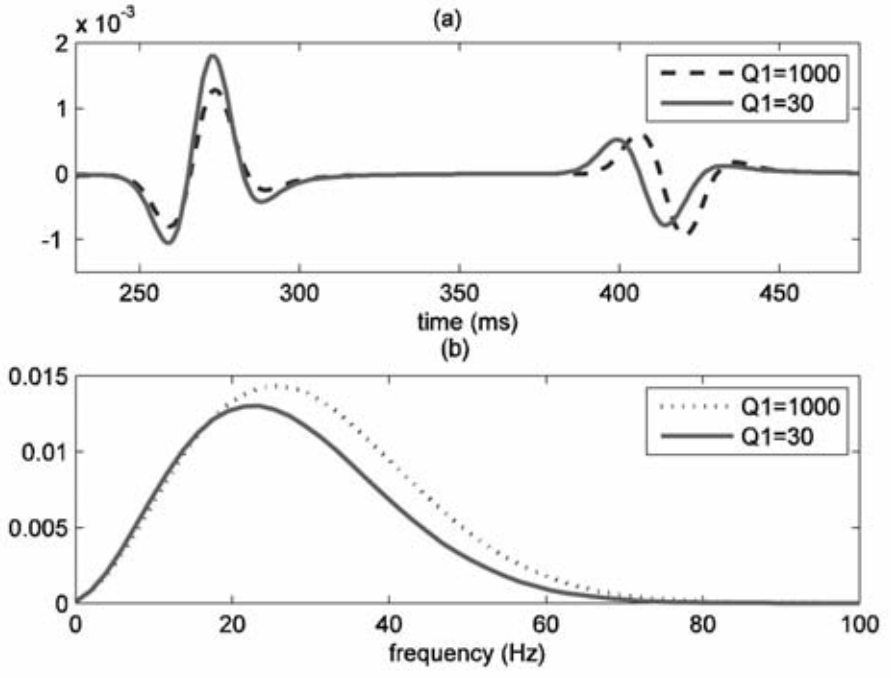

Fig. 7. (a) Traces for offset 100 m with $Q_1 = 1000$ (dashed) and $Q_1 = 30$ (solid). (b) The amplitude spectrums of the reflected waves form the second interface for $Q_1 = 1000$ (dashed) and $Q_1 = 30$ (solid).

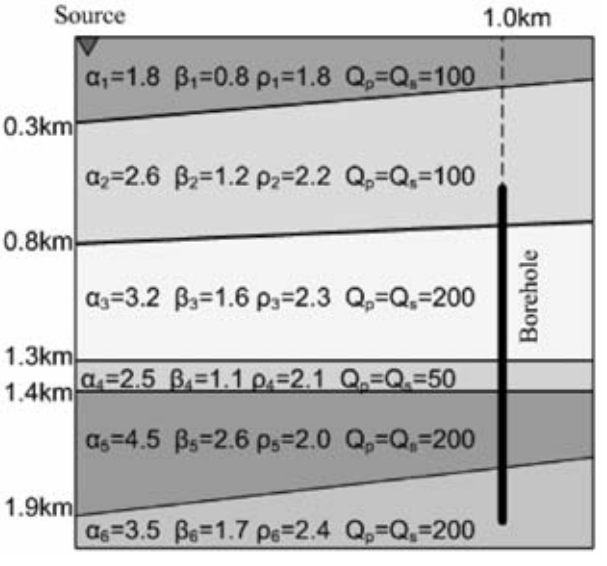

Fig. 8. Viscoelastic layered model with five interfaces.

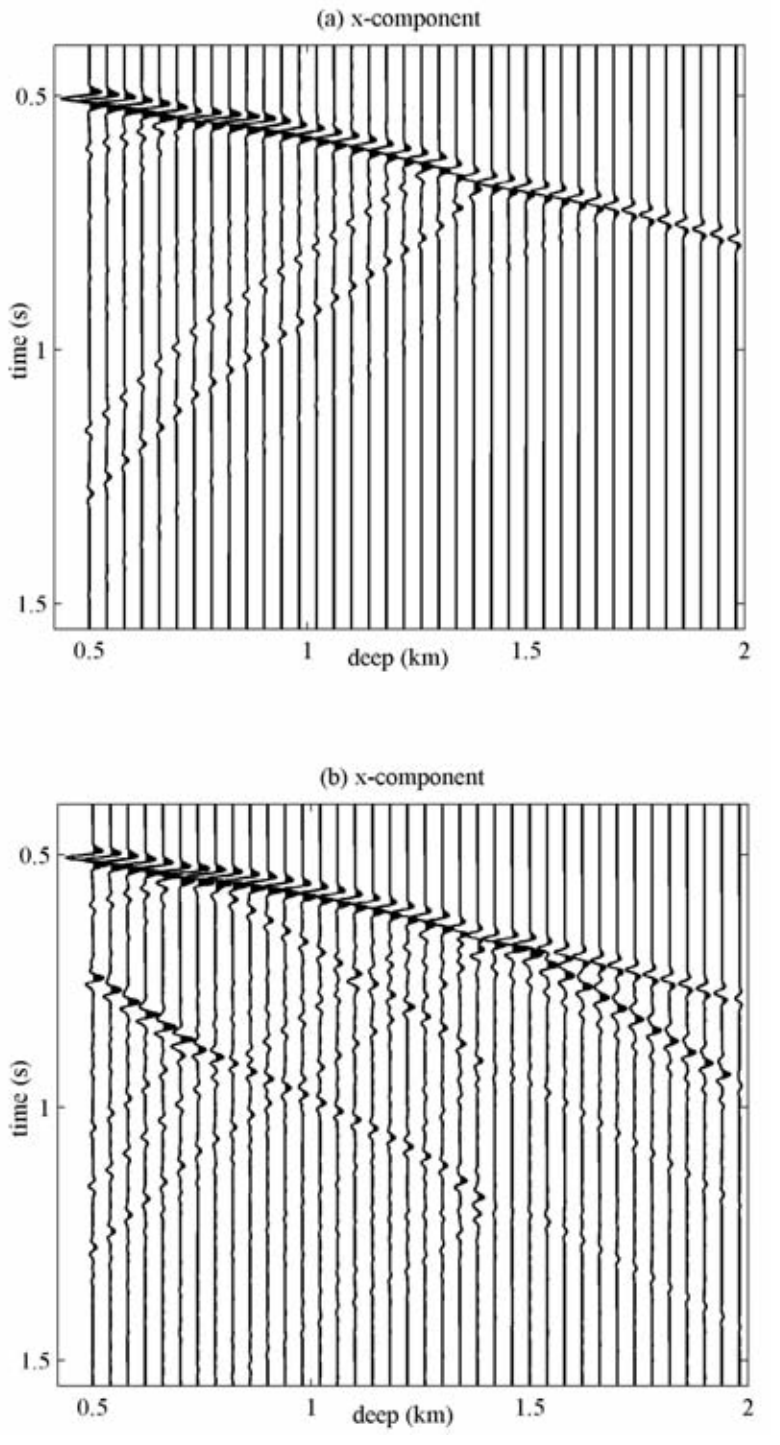

Fig. 9. The synthetic VSP seismograms with our method (a) and finite difference method (b).

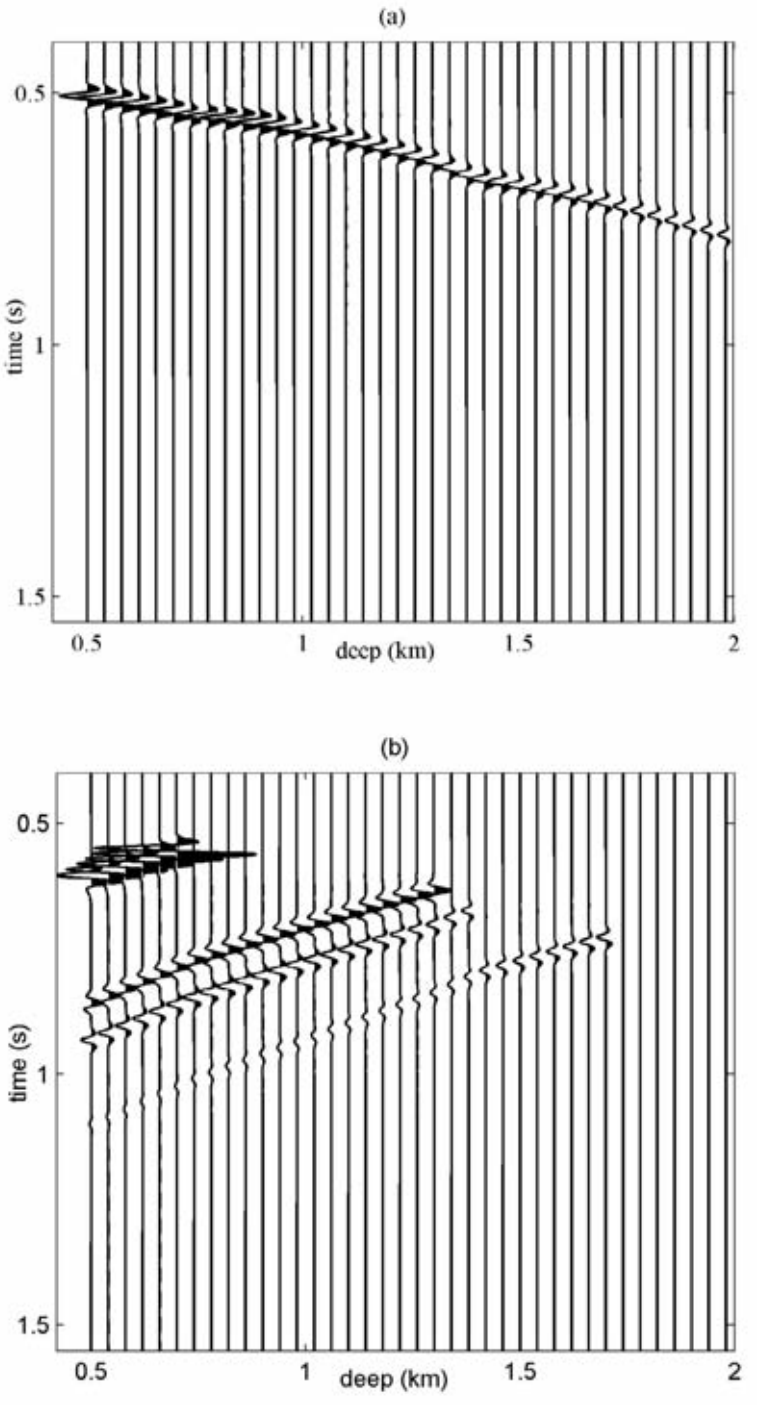

Fig. 10. The x-component of some partial VSP wavefields are generated respectively with our method: (a) the direct waves, (b) primary reflected P-waves.

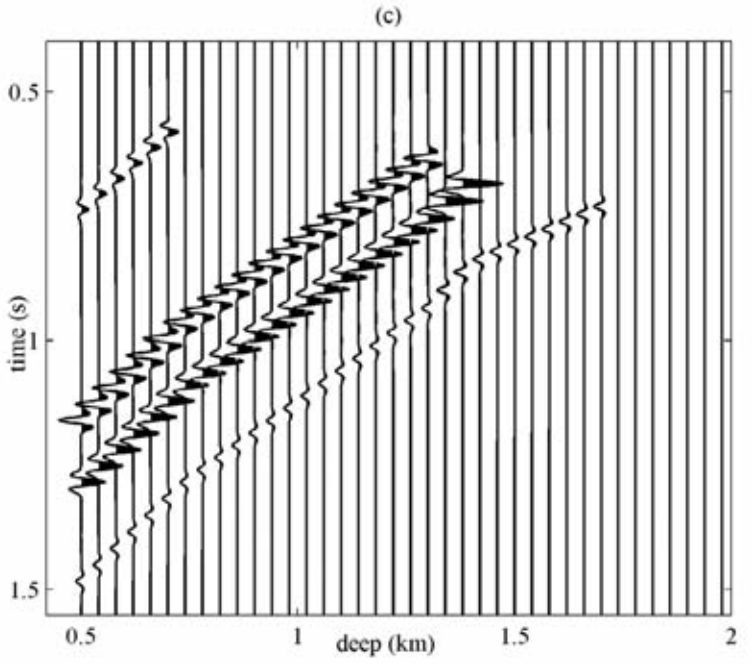

Fig. 10. The x-component of some partial VSP wavefields are generated respectively with our method: (c) the converted P-S waves.

Subsequently, the receivers are set at the surface. Fig. 11 shows the x-component of the primary P-S reflections. The P-S head wave is generated automatically. In this example, the integral interval of horizontal slowness is , $[-1/\alpha_1 \ \ 2/\alpha_1]$, integral step is 0.002 s/m, bandwidth of frequency is $0 \sim 100$ Hz and frequency interval is 0.45 Hz. The runtime of our method is about 100 s. For the rotated staggered-grid finite difference method with perfectly matched layer-absorbing boundary conditions, if we take the spacing interval as 4 m (625×500 grid) and time interval as 0.5 ms, the runtime is about 800 s. Both computations were made using an Intel Pentium D 2.8 GHz processor with 2GB RAM. Thus, our method is more efficient than the finite difference method, especially for the media with thick layers and strong contrast.

CONCLUSIONS

A one-way method is proposed to simulate the wave propagation in layered viscoelastic media with dipping interfaces. The dipping angle of each interface can be arbitrary as long as the interfaces do not cross each other.

Synthetic seismograms show that the new method is quite accurate and can model the changes in amplitude and phase caused by Q. Our method is more efficient in computation time and more suited for the media with thick layer and strong contrast when compared with the finite difference method. Another advantage of our method is its flexibility. It can separately simulate various partial wavefields; for example, the primary reflected P-waves or primary reflected S-waves, the P-S or S-P converted waves, and the multiples that are of interest to us. The components of the partial wave field that we hope to model can be coded as a chain of characters that are similar to the ray code. Then, at each interface, a secondary wave (reflected or transmitted and P or S) can be chosen according to this code. Our method has potential applications in seismic interpretation or inversion of seismic attributes.

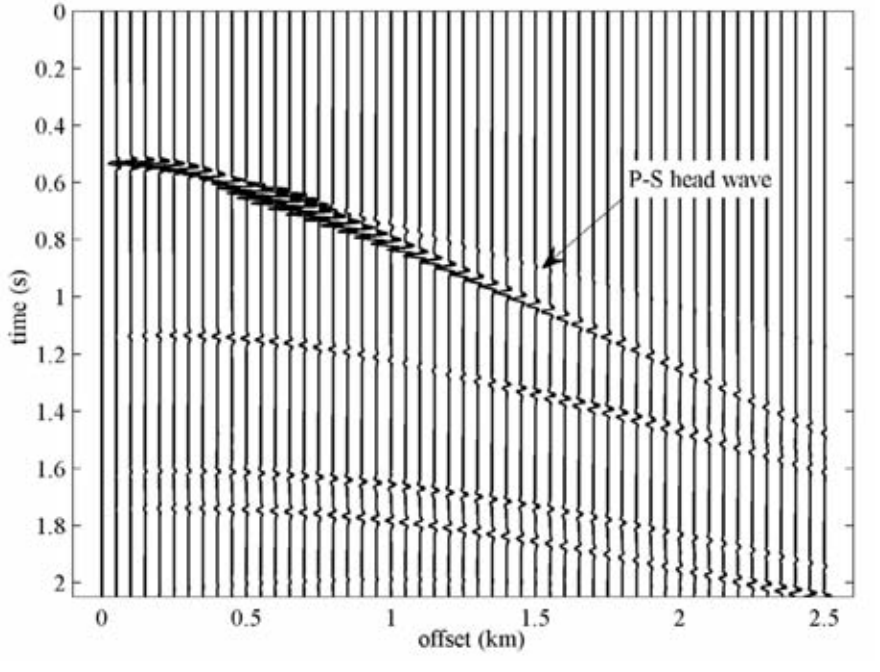

Fig. 11. The synthetic P-S primary reflections with our method. The head wave is also generated.

ACKNOWLEDGEMENTS

This work was supported by the National Natural Science Foundation of China (40730424, 40674064), National 863 Program (2006A09A102) and National Science & Technology Major Project (2008ZX05023-005-005, 2008ZX05025-001-009, 2011ZX05023-005, 2011ZX05023-005).

REFERENCES

Aki, K. and Richards, P., 2002. Quantitative Seismology. University Science Books, New York.

Becache, E., Ezziani, E. and Joly, P., 2004. A mixed finite element approach for viscoelastic wave propagation. Computat. Geoscien., 8: 255-299.

Berkhout, A.J., 1982. Seismic Migration, Imaging of Acoustic Energy by Wave Field Extrapolation. Elsevier Science Publishers, Amsterdam.

Bourbie, T., 1983. Synthetic seismograms in attenuating media. Geophysics, 48: 1575-1587.

Carcione, J.M. and Hermann, G.C., 2002. Seismic modeling. Geophysics, 67: 1304-1325.

Červený, V., 2001. Seismic Ray Theory. Cambridge University Press, Cambridge.

Chapman, C.H., 1978. A new method for computing seismograms. Geophys. J. Roy. Astron. Soc., 54: 481-518.

Chen, X.F., 1990. Seismogram synthesis for multi-layered media with irregular interfaces by global reflection/transmission matrices method, I - Theory of 2-D SH case. Bull. Seismol. Soc. Am., 80: 1696-1724.

Chen, X.F., 1996. Seismogram synthesis for multi-layered media with irregular interfaces by global generalized reflection/transmission matrices method, III - Theory of 2D P-SV Case. Bull. Seismol. Soc. Am., 86: 389-405.

Frazer, L.N. and Gettrust, J.F., 1984. On a generalization of Filon's method and the computation of oscillatory integrals of seismology. Geophys. J. Roy. Astron. Soc., 76: 461-481.

Fuchs, K. and Müller, G., 1971. Computation of synthetic seismograms by the reflectivity method and comparison with observations. Geophys. J. Roy. Astron. Soc., 23: 417-433.

Ge, Z.I. and Chen, X.F., 2007. Wave propagation in irregularly layered elastic models: a boundary element approach with a global reflection/transmission matrix propagator. Bull. Seismol. Soc. Am., 97: 1025-1031.

Kennett, B.L.N., 1983. Seismic Wave Propagation in Stratified Media. Cambridge University Press, Cambridge.

Krebes, E.S. and Daley, P.F., 2007. Difficulties with computing anelastic plane-wave reflection and transmission coefficients. Geophys. J. Internat., 170: 205-216.

Kroode, F.T., 2002. Prediction of internal multiples. Wave Motion, 35: 315-338.

Martin, K. and Michael, D., 2006. An arbitrary high-order discontinuous Galerkin method for elastic waves on unstructured meshes - I. The two-dimensional isotropic case with external source terms. Geophys. J. Internat., 166: 855-877.

Müller, G., 1985. The reflectivity method: a tutorial. J. Geophys., 58: 153-174.

Stekl, I. and Pratt, R.G., 1998. Accurate viscoelastic modeling by frequency-domain finite differences using rotated operators. Geophysics, 63: 1779-1794.

Steven, R. and Robert, H.W., 1989. Amplitude versus offset variation in gas sands. Geophysics, 54: 680-688.

Toverud, T. and Ursin, B., 2005. Comparison of seismic attenuation models using zero-offset vertical seismic profiling (VSP) data. Geophysics, 70: 17-25.